

## Long-Term Memory Deficits in Pavlovian Fear Conditioning in $\text{Ca}^{2+}$ /Calmodulin Kinase Kinase $\alpha$ -Deficient Mice<sup>∇</sup>

Frank Blaeser,<sup>1</sup> Matthew J. Sanders,<sup>2</sup> Nga Truong,<sup>3</sup> Shanelle Ko,<sup>4</sup> Long Jun Wu,<sup>4</sup>  
David F. Wozniak,<sup>5</sup> Michael S. Fanselow,<sup>2</sup> Min Zhuo,<sup>4</sup> and Talal A. Chatila<sup>3\*</sup>

*Institute of Transfusion Medicine, University of Leipzig, Leipzig, Germany<sup>1</sup>; Department of Psychology, University of California at Los Angeles, Los Angeles, California 90095<sup>2</sup>; Department of Pediatrics, The David Geffen School of Medicine, University of California at Los Angeles, Los Angeles, California 90095<sup>3</sup>; Department of Physiology, University of Toronto, Toronto, Ontario, Canada M5S 1A8<sup>4</sup>; and Department of Psychiatry, Washington University School of Medicine, St. Louis, Missouri 63110<sup>5</sup>*

Received 6 August 2006/Returned for modification 29 August 2006/Accepted 18 September 2006

**Signaling by the  $\text{Ca}^{2+}$ /calmodulin kinase (CaMK) cascade has been implicated in neuronal gene transcription, synaptic plasticity, and long-term memory consolidation. The CaM kinase kinase  $\alpha$  (CaMKK $\alpha$ ) isoform is an upstream component of the CaMK cascade whose function in different behavioral and learning and memory paradigms was analyzed by targeted gene disruption in mice. CaMKK $\alpha$  mutants exhibited normal long-term spatial memory formation and cued fear conditioning but showed deficits in context fear during both conditioning and long-term follow-up testing. They also exhibited impaired activation of the downstream kinase CaMKIV/Gr and its substrate, the transcription factor cyclic AMP-responsive element binding protein (CREB) upon fear conditioning. Unlike CaMKIV/Gr-deficient mice, the CaMKK $\alpha$  mutants exhibited normal long-term potentiation and normal levels of anxiety-like behavior. These results demonstrate a selective role for CaMKK $\alpha$  in contextual fear memory and suggest that different combinations of upstream and downstream components of the CaMK cascade may serve distinct physiological functions.**

$\text{Ca}^{2+}$ -regulated signaling pathways play a pivotal role as mediators of various forms of synaptic plasticity and behavioral responses. A major mechanism by which  $\text{Ca}^{2+}$  regulates neuronal functions involves activation of a  $\text{Ca}^{2+}$ /calmodulin-dependent protein kinase (CaMK) cascade composed of upstream activator kinases and downstream effector kinases (reviewed in references 9 and 47). The activity of downstream kinases of this cascade, including CaMKI and CaMKIV/Gr, is greatly enhanced by *trans*-phosphorylation by CaMK kinases (CaMKK). Two CaMKK have been identified, CaMKK $\alpha$  and CaMKK $\beta$  (2, 10, 49). CaMKK $\alpha$  and CaMKK $\beta$  being products of distinct genes (*Camkk1* and *Camkk2*, respectively), these CaM kinases bind to and are activated by the same allosteric regulator,  $\text{Ca}^{2+}$ /calmodulin, also required for activation of their downstream substrates CaMKI and CaMKIV/Gr. Both CaMKK appear similarly capable of phosphorylating and activating both CaMKI and CaMKIV/Gr (2, 10, 49). CaMKK $\alpha$  and  $\beta$  are both enriched in the brain and exhibit a neuronal expression profile that strongly overlaps with those of CaMKI and CaMKIV/Gr (2, 42, 44). CaMKK immunoreactivity has been found in both the cytosol and nucleus.

Effector components of the CaMK cascade have been implicated in key neuronal functions. CaMKIV/Gr is a major mediator of  $\text{Ca}^{2+}$ -dependent gene transcription in neurons both by virtue of its nuclear localization and its capacity to activate several transcriptional regulators (53). These include the transcription factor CREB, which it phosphorylates on the

regulatory Ser133 residue, the CREB-related factor ATF-1, the MADS-box family members SRF and MEF2, and the transcriptional coactivator p300/CREB-binding protein (CBP) (5, 8, 20, 22, 35–37, 48). CaMKI is localized primarily in the cytosol and has been shown to regulate axonal extension and growth cone motility and to promote long-term potentiation (LTP) by extracellular signal-regulated kinases (44, 51).

Genetic models have begun to clarify the function of different components of the CaMK cascade. In the nematode *Caenorhabditis elegans*, there exists a simple two-component CaMK cascade composed of an upstream CaMKK homologue and a downstream CaMKI homologue. Transgenic and gene disruption approaches revealed that the *Caenorhabditis elegans* CaMK cascade activates CREB- and CRE-mediated transcription in neurons in vivo (27). The larger number of component kinases found in the mammalian CaMK cascade has been associated with a more complex picture that has emerged from targeted gene disruption studies in mice. CaMKIV/Gr knockout (KO) mice exhibited profound deficits in CREB activation in the context of behavioral paradigms, including restraint stress response and classical fear conditioning (18, 41). CaMKIV/Gr-deficient mice also exhibited deficits in several forms of synaptic plasticity relevant to learning and memory, and they suffered from a striking loss of long-term fear memory, including cued and contextual fear memory (18, 52). Targeted disruption of CaMKK $\beta$  resulted in impairment of spatial training-induced CREB activation and spatial memory formation (38). However, unlike CaMKIV/Gr deficiency, CaMKK $\beta$  deficiency did not influence fear memory formation (38). In turn, CaMKIV/Gr deficiency did not impact spatial memory formation (18). This suggests that combinations of upstream and downstream components of the CaMK cascade might act in a nonredundant manner to mediate effector functions.

\* Corresponding author. Mailing address: Department of Pediatrics, The David Geffen School of Medicine, University of California at Los Angeles, 10833 Le Conte Avenue, Los Angeles, CA 90095-1752. Phone: (310) 825-4125. Fax: (310) 206-4584. E-mail: Tchatila@mednet.ucla.edu.

<sup>∇</sup> Published ahead of print on 2 October 2006.

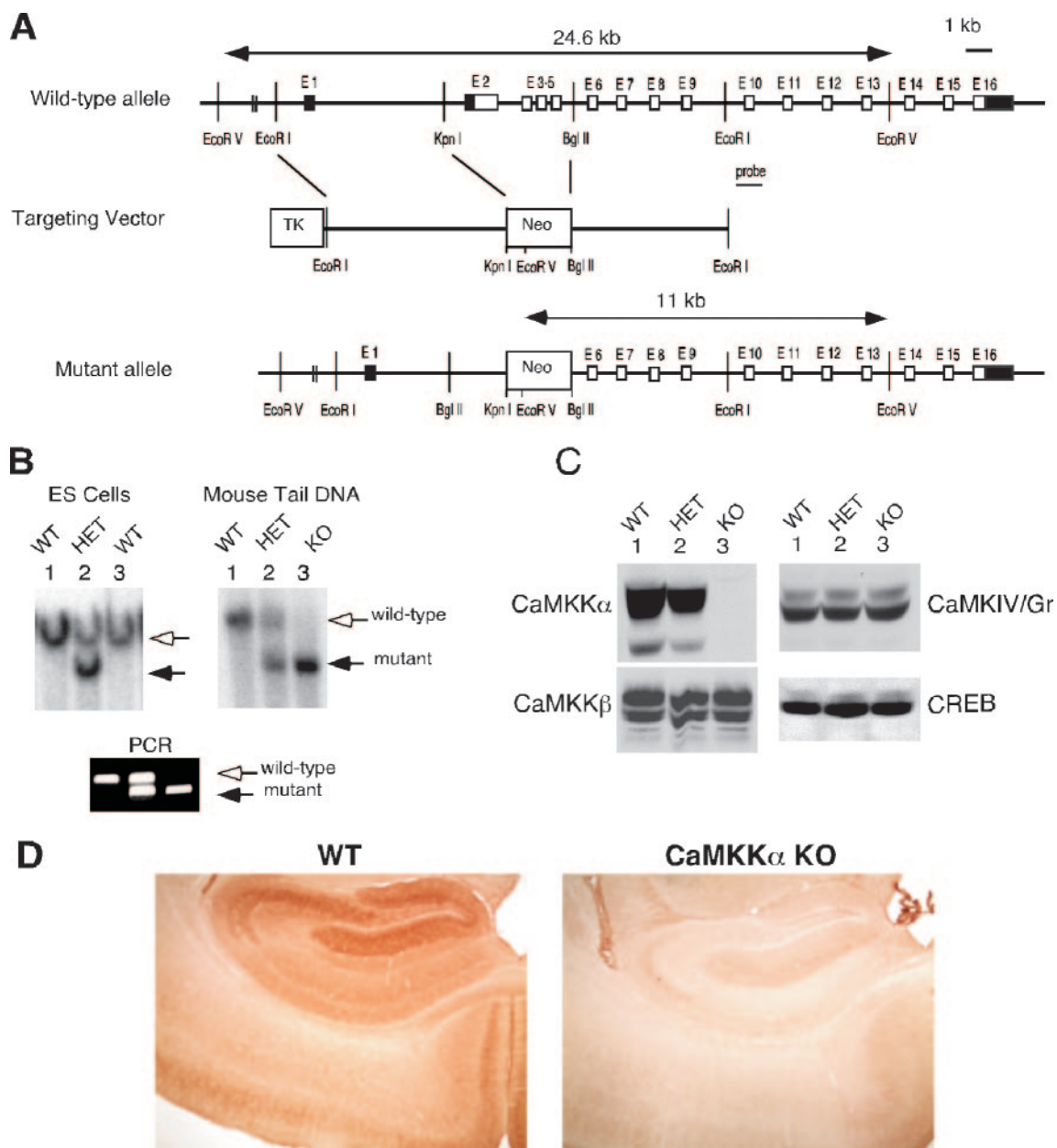


FIG. 1. Targeted disruption of the murine CaMKK $\alpha$  gene. (A) Targeting strategy. Exons 2 to 5 of *Camkk1*, encoding the catalytic domain of CaMKK $\alpha$ , were replaced with a *neo* cassette. The introduction by homologous recombination of an EcoRV site found within the *neo* cassette converts a 23-kb EcoRV genomic fragment spanning exons 1 to 13 of the WT *Camkk1* allele into a 11-kb fragment in the mutant allele. TK denotes the herpes simplex virus thymidine kinase gene that was used for negative selection with ganciclovir. E1, exon 1. (B) Southern blot analysis (top panels) of ES cells and mouse tail DNA digested with EcoRV and subjected to hybridization using a genomic DNA probe 3' to the targeting construct (depicted in panel A). The WT and mutant alleles give rise to 24.6- and 11-kb bands, respectively. (Bottom) PCR analysis of WT and mutant alleles using primers both flanking and within the *neo* cassette. The WT and mutant alleles give rise to 475- and 290-bp products, respectively. (C) Immunoblot analysis of CaMKK $\alpha$ , CaMKK $\beta$ , CaMKIV/Gr, and CREB expression in the brains of WT, HET, and KO mice. (D) Immunohistochemical analysis of CaMKK $\alpha$  expression in the hippocampus showing the absence of CaMKK $\alpha$  expression in mutant mice compared to WT littermate controls.

To further investigate the *in vivo* function of different components of the CaMK cascade, we generated mice that are deficient in CaMKK $\alpha$  by homologous gene recombination. We found that CaMKK $\alpha$ -deficient mice exhibited defective CaMKIV/Gr and CREB activation immediately following fear conditioning. They also showed performance deficits during

fear conditioning and during several subsequent contextual fear tests conducted over time.

#### MATERIALS AND METHODS

**Generation of *Camkk1* null mutants.** The *Camkk1* gene is spread over a 23-kb stretch and contains 16 exons (Fig. 1). Exon 1 and part of exon 2 are noncoding,

while exon 16 contains the stop codon and 3' untranslated region. A targeting construct was designed to replace exons 2 to 5 with a neomycin gene cassette (Fig. 1). A 6-kb EcoRI/KpnI fragment 5' to the targeted sequence was cloned into the targeting vector pPNT, containing both positive (neomycin) and negative (thymidine kinase) selection genes, to create the 5' homology region of the targeting construct. A 5-kb BglII/EcoRI fragment was used as a 3' homology region of the construct. RW4 embryonic stem (ES) cells were transfected and then subjected to positive (neomycin analogue G418) and negative (ganciclovir) selection. Doubly resistant clones were screened for homologous gene recombination by Southern blotting. DNA was digested with EcoRV and probed with a 1-kb EcoRI/ClaI fragment immediately distal to the 3' homology sequence. Successful recombination gave rise to a band of approximately 11 kb, in contrast to an approximately 20-kb band for the wild-type (WT) allele.

Heterozygous (HET) CaMKK $\alpha$ -deficient ES cells were injected into C57BL/6 blastocysts, which were reimplanted in pseudopregnant females. Several male chimeras were identified by agouti coat color, and those showing more than 80% agouti coats were mated to C57BL/6 females. Agouti offspring were screened for heterozygosity by Southern blot and PCR analyses, and heterozygous animals were bred to generate homozygous CaMKK $\alpha$ -deficient mice (Fig. 1). Complete CaMKK $\alpha$  deficiency was confirmed by immunoblotting with anti-CaMKK $\alpha$  antibodies (Fig. 1). PCR genotyping was done using the following primers: 5'-GG TTGTCAGCAGAGGTAGC-3' (common sense primer; located in intervening sequence 1 of the murine CaMKK $\alpha$  gene bp 444 of GenBank accession number AF461702.1), 5'-GTTTTTCTCTTGATCCAC-3' (WT antisense primer; located in intervening sequence 1 901 rev of GenBank accession number AF461702.1), and 5'-ACTGGCTTCACATTCCT-3' (located in the inserted neomycin resistance cassette). The presence of the WT allele is associated with amplification of a 475-bp DNA fragment, while the mutant allele gives rise to a 290-bp product.

The mice used in these studies were housed on a 12-h light/12-h dark cycle with ad libitum access to rodent chow. All the respective experimental protocols were conducted in accordance with National Institutes of Health guidelines and were approved by the Animal Care and Use Committees of Washington University School of Medicine, the University of California at Los Angeles, and the University of Toronto.

**Histological and immunohistochemical analyses.** For histological analysis, freshly dissected brains of adult KO mice and WT littermate controls were fixed overnight in phosphate-buffered 4% paraformaldehyde, embedded, and cut into 10- $\mu$ m sections which were subjected to Giemsa staining following standard procedures. For immunohistochemistry, paraformaldehyde-fixed brains were cryoprotected for 48 h in 10% sucrose in phosphate-buffered saline. Immunohistochemical analysis was performed on free-floating sections cut at 35  $\mu$ m on a cryostat. After the sections were blocking in 3% normal goat serum in Dulbecco's phosphate-buffered saline for 30 min, they were incubated with one of the following primary antibodies, as indicated: polyclonal rabbit anti-CaMKK $\alpha$  antibody (1:400 dilution), anti-pCaMKIV/Gr antibody (1:50 dilution) (Santa Cruz Biotech), or polyclonal rabbit anti-pCREB antibody (1:500 dilution; New England Biolabs). Immunoreactivity was visualized using a peroxidase Vectastain Elite ABC kit (Vector Laboratories). Staining intensity was quantified utilizing ImageJ software and analyzed for statistical significance between genotypes by Student's two-tailed *t* test.

**Immunoblotting.** Tissue homogenates were derived from dissected brains and testes of adult WT, HET, and KO littermate mice using a Polytrone homogenizer. Homogenates were cleared by high-speed centrifugation, and 50  $\mu$ g protein samples were resolved by sodium dodecyl sulfate-polyacrylamide gel electrophoresis and then transferred to nitrocellulose membranes for immunoblotting. Membranes of whole-brain homogenates or neuronal cell culture lysates were blocked in fat-free milk and then probed with one or more of the following antibodies as indicated. Rabbit polyclonal anti-CaMKK $\alpha$  and anti-CaMKK $\beta$  antibodies and mouse monoclonal anti-CREB antibody were obtained from Santa Cruz Biotechnology, and mouse monoclonal anti-CaMKIV/Gr catalytic domain antibody was from Pharmingen. The blots were developed using horseradish peroxidase-conjugated secondary antibodies and enzyme-linked chemiluminescence (ECL kit; Amersham).

**Electrophysiological studies in hippocampal slices.** The electrophysiological experiments were carried out following previously established procedures (18). Male adult WT and CaMKK $\alpha$  KO mice (15 to 16 weeks old) were anesthetized with inhaled isoflurane. For field potential recordings, transverse slices (400  $\mu$ m) of hippocampus were rapidly prepared and maintained in an interface chamber at 28°C, where they were suffused with artificial cerebrospinal fluid (ACSF), consisting of 124 mM NaCl, 4.4 mM KCl, 2.0 mM CaCl<sub>2</sub>, 2.0 mM MgSO<sub>4</sub>, 25 mM NaHCO<sub>3</sub>, 1.0 mM NaH<sub>2</sub>PO<sub>4</sub>, and 10 mM glucose, bubbled with 95% O<sub>2</sub> and 5% CO<sub>2</sub>. The protocol of electrical stimulation and recordings has been described

previously (28, 31, 52). Slices were kept in the recording chamber for at least 2 h before the experiments. A bipolar tungsten stimulating electrode was placed in the stratum radiatum in the CA1 region, and extracellular field potentials were also recorded in the stratum radiatum using a glass microelectrode (3 to 12 M $\Omega$ , filled with ACSF). Stimulus intensity was adjusted to produce a response of ~1-mV amplitude. Test responses were elicited at 0.02 Hz. LTP was induced using two tetanic train stimulations (100 Hz, 1-s trains at a 20-s interval).

For whole-cell recordings, slices (300  $\mu$ m) were cut using a Vibratome tissue slicer and were transferred to a submerged recovery chamber containing oxygenated (95% O<sub>2</sub> and 5% CO<sub>2</sub>) ACSF with a lower concentration of KCl (2.5 mM) for at least 1 h before the experiments. Experiments were performed in a recording chamber on the stage of an Axioskop 2FS microscope with infrared differential interference contrast optics for visualizing whole-cell patch clamp recordings. Stimulation was delivered by a bipolar tungsten stimulating electrode placed in the stratum radiatum in the CA1 region. CA1 neurons were voltage clamped at -30 mV, and *N*-methyl-D-aspartate (NMDA) receptor-mediated excitatory postsynaptic currents (EPSCs) were measured after the blockade of L- $\alpha$ -amino-3-hydroxy-5-methyl-4-isoxazolepropionic acid (AMPA)/kainate receptors using 20  $\mu$ M 6-cyano-7-nitroquinoxaline-2,3-dione (CNQX). The NMDA receptor-mediated EPSCs were completely blocked by 50  $\mu$ M AP-5, supporting NMDA receptor-mediated responses.

Group data are presented in the figures as means  $\pm$  standard errors of the means. Two-way analysis of variance (ANOVA) and Student's *t* test were used for statistical analysis. A *P* value of <0.05 was considered significant.

**Behavioral studies. (i) Genetic background of tested animals.** All behavioral tests were carried out on 12- to 16-week-old male mice. F<sub>2</sub> hybrid siblings were used for the Morris water maze test, while fear conditioning and the elevated plus maze test were carried out on CaMKK $\alpha$  KO mice that were backcrossed for 10 or 11 generations on C57BL/6 mice (Charles River). WT control mice were littermates derived from matings of heterozygous animals. The mice were housed on a 12-h light/12-h dark cycle (lights on 6 a.m.) with ad libitum access to rodent chow. All behavioral testing occurred during the light portion of the cycle. All mouse protocols were conducted in accordance with NIH guidelines and approved by the Animal Care and Use Committee.

**(ii) Open field activity.** To record horizontal locomotor activity, we used the Activity Monitor system from Med Associates (43.2  $\times$  43.2  $\times$  30.5 cm; Med Associates, St. Albans, VT). Briefly, this system uses paired sets of photo beams to detect movement in the open field, and movement is recorded as beam breaks. The open field was placed inside an isolation chamber with dim illumination and a fan. Each subject was placed in the center of the open field, and activity was measured for 30 min.

**(iii) Fear conditioning.** Each mouse was trained in one of four identical conditioning chambers. Animals were run with their cage mates, in squads of two to four animals. These chambers were also used for context tests after conditioning. The chambers were situated on a stainless steel rack in a brightly lit room. Each chamber was cubic (30 cm  $\times$  24 cm  $\times$  21 cm; Med Associates, Inc., St. Albans, VT) and had a white opaque back wall, aluminum sidewalls, and a clear polycarbonate front door. Each chamber had a removable grid floor and waste pan. Between each successive squad of mice, the boxes were cleaned with a 1% acetic acid solution and dried thoroughly. A thin film of the acetic acid solution was placed in the waste pan before the introduction of each squad. The grid floor contained 36 stainless steel rods (3-mm diameter) spaced 8 mm center to center. When placed in the chamber, the grid floor made contact with a circuit board through which scrambled shock was delivered. During training and context testing, a standard HEPA filter provided background white noise of 55 dB.

To assess cued fear conditioning, tone testing was conducted in distinct chambers in another room in the laboratory. These chambers were placed on a stainless steel rack in a dimly lit room. Each chamber was constructed with the same dimensions as those used for training but contained no grid floor or waste pan. In addition, a white curved sheet of Plexiglas was inserted into each chamber to create a semicylindrical space. No background noise was established during tone testing.

On the conditioning day, individual boxes were carried from the vivarium to the laboratory. Each mouse was placed in a chamber and allowed 2 min of exploration before the delivery of any stimuli. Beginning at the 2-min mark, three tone-shock pairings were delivered. The tone was 30 s in duration, 2,800 Hz in frequency, and 85 dB in intensity. At the end of each tone, a shock was delivered at 0.75-mA intensity and 2-s duration. Tone-shock pairings were delivered at a 30-s intertrial interval. Animals were removed from the chambers 30 s after the third shock. Postshock freezing was recorded during the 30-s period following each shock. These data were used as a measure of short-term context conditioning (11).

On context testing days, each mouse was placed into a chamber for 5 min. Freezing was recorded throughout the 5-min test. On cued testing days, each

mouse was placed into a chamber and allowed 2 min of exploration before the delivery of the tone. At the 2-min mark, a single 3-min tone was presented. Freezing was recorded during both the 2-min baseline period and the 3-min tone period.

Throughout all training and testing, the presentation of tone and shock stimuli was controlled by a personal computer running Med Associates software (MedAssociates, Inc., St. Albans, VT). A single camera in each context recorded the behavior of animals in four chambers. Freezing was measured with an automated system whereby continuous video data were analyzed with the aid of NIH Image. This system has been described in detail elsewhere (1). It measures the variance in pixel intensity across successive video frames (taken at 1 Hz) and then computes its standard deviation. A threshold is then applied to the data to yield a percent freezing score. In pilot experiments (data not shown), the threshold for freezing was adjusted to yield 98% agreement with a pair of human observers. The mean percent freezing score (averaged across a 5-min context test or across a 3-min tone test) served as the dependent measure for analyses. We employed a mixed ANOVA design, with genotype as a between-subjects factor and repeated context or tone tests as a within-subjects factor and with  $P < 0.05$  set as the criterion for statistical significance.

**(iv) Morris water navigation test.** Spatial learning and memory capabilities were evaluated by the Morris water maze test using a protocol similar to previously published methods (18). Briefly, this involved testing mice in a round pool (100-cm inner diameter) filled with opaque water on a cued (visible platform, variable location), place (submerged platform, fixed location), and probe (platform removed) trials. The navigation of the mice was tracked by a video camera, and the escape latency and distance traveled (path length) to reach the platform were recorded. Swimming speeds were calculated as well. Testing on the cued condition was carried out using blocks of four trials/session/day over a 2-day period for a total of 8 trials. Trial sessions consisted of two sets of two consecutive 60-s trials separated by 1 h of rest. The platform was moved for each trial. Data were analyzed in blocks of two trials each. The protocol used for assessing acquisition during place trials involved two consecutive trials per day over a period of 10 days of testing using an intertrial interval of 60 s. The submerged platform was randomly assigned to one of the four pool quadrants (north, south, east, and west) where it remained in the same location for all trials. Release points (northeast, southeast, southwest, and northwest) were pseudorandomly assigned with one point being used for each trial within a block of four trials, and the same release point was never used for two consecutive trials. Data were analyzed in blocks of four trials so that data from each release point were represented. Approximately 1 h after the second trial on day 5 and day 10, the mice were evaluated in a probe trial, during which the escape platform was removed from the pool and a mouse was released into the maze in a quadrant that was opposite the one which had contained the platform. Time spent searching in the target quadrant in which the platform had been located and the number of crossings made over the former platform location (platform crossings) were recorded. An ANOVA model containing one between-subjects factor, genotype (CaMKK $\alpha$  KO versus WT), and one within-subjects factor, blocks of trials, or trials, was used to analyze the water navigation data.

**(v) Elevated plus maze.** Animal cages were transferred individually from the vivarium to the room containing the elevated plus maze. The maze was constructed of wooden floors (four arms, each measuring 7.6 cm in width and 28 cm in length) sealed with vinyl stripping and painted beige. Two of the arms were flanked by black Plexiglas walls (each 16.5 cm tall). The center quadrant (7.6 cm  $\times$  7.6 cm) of the maze was not walled. The maze was situated on a tripod at approximately 60 cm from the ground. Each mouse was placed in the center of the maze and allowed to explore freely for 5 min. An overhead camera recorded the behavior of each animal, and video records were made on VHS tape. The tapes were scored later by an experimenter blind to the genotype of each subject. The total amount of time spent in the open portion of the maze (including the center) was analyzed as the dependent measure. A simple  $t$  test was used to evaluate differences among genotypes, with  $P < 0.05$  set as the criterion for statistical significance.

**Nucleotide sequence accession numbers.** The sequences of the 16 exons of the *Camkk1* gene and their surrounding intronic sequences have been deposited in GenBank (accession numbers AF461701, AF461702, AF461703, AF461704, AF461705, and AF461706).

## RESULTS

**Generation of CaMKK $\alpha$ -deficient mice.** The targeting strategy aimed to disrupt CaMKK $\alpha$  expression by replacing exons 2 to 5 of *Camkk1* with a neomycin resistance cassette (Fig. 1A).

The targeted exons encode amino acids 1 to 171 of the kinase, including the amino acids involved in ATP binding of the catalytic domain (subdomains I and II by the numbering system of Hanks et al. [16]) and the N-terminal 5 amino acids of the arginine-proline-rich insert sequence. Four of 137 G418- and ganciclovir-resistant ES clones underwent homologous recombination as determined by Southern blot analysis employing a hybridization probe external to the region of homology contained within the targeting vector. Several male chimeras were generated from the ES clones which transmitted the mutant allele through the germ line. Matings of HET mice resulted in generation of CaMKK $\alpha$  KO mice (Fig. 1B). Immunoblot analysis using several different antibodies directed at the amino- and carboxyl-terminal sequence of the protein revealed the absence of CaMKK $\alpha$  in KO mice, consistent with a null phenotype (Fig. 1C). Levels of other components of the CaMK cascade, including CaMKK $\beta$  and CaMKIV/Gr and the downstream target CREB, were unaltered (Fig. 1C). Immunohistochemical analysis confirmed the absence of CaMKK $\alpha$  immunoreactivity in different regions of the brain (Fig. 1D). CaMKK $\alpha$  KO mice were generated in numbers consistent with autosomal recessive Mendelian inheritance (data not shown). KO mice of both sexes were grossly indistinguishable from their WT and HET littermates and were fertile.

**Normal spatial memory in CaMKK $\alpha$ -deficient mice.** The data from the cued trials showed that the CaMKK $\alpha$  KO and WT mice performed similarly in terms of escape path length (Fig. 2A) and latency (data not shown). Specifically, ANOVAs conducted on these data yielded nonsignificant effects of genotype, for both path length and latency ( $F_{1,25} < 1$  for both) as well as nonsignificant genotype by blocks of trials interactions ( $F_{3,75} = 1.61$  and  $P > 0.1$  and  $F_{3,75} = 1.41$  and  $P > 0.1$ , respectively). These results suggested that nonassociative influences (e.g., sensorimotor or visual disturbances and alterations in motivation) were not likely to have affected the performance of the CaMKK $\alpha$  KO mice and thus would not confound interpretation of learning capabilities evaluated during subsequent place trials. Acquisition performance during the place trials also appeared to be similar between the CaMKK $\alpha$  KO and WT mice in terms of both path length (Fig. 2B) and latency (data not shown). For example, ANOVAs performed on the place trial data showed a nonsignificant effect of genotype for both path length and latency during acquisition ( $F_{1,25} < 1$  for both), and the effect of genotype by blocks of trials interactions were also nonsignificant for both variables ( $F_{4,100} < 1$  for both). Similarly, an ANOVA conducted on swimming speed during the place trials also revealed a nonsignificant effect of genotype ( $F_{1,25} = 1.17$  and  $P > 0.1$ ) and a nonsignificant effect of genotype by blocks of trials interaction ( $F_{4,100} = 1.30$  and  $P > 0.1$ ), thus documenting a lack of differences between the groups on this variable (not shown). The similar swimming speeds of the two groups suggested that the swimming capabilities of the CaMKK $\alpha$  KO mice were not compromised and thus did not affect their acquisition performance. ANOVAs conducted on the probe trial data (Fig. 2C and D) showed that the retention performance of the CaMKK $\alpha$  KO and WT mice was also similar in terms of time spent in the target quadrant (effect of genotype and effect of genotype by probe test interaction,  $F_{1,25} = 1.34$  and  $P = 0.26$  and  $F_{1,25} < 1$ , respectively) and platform crossings (effect of geno-

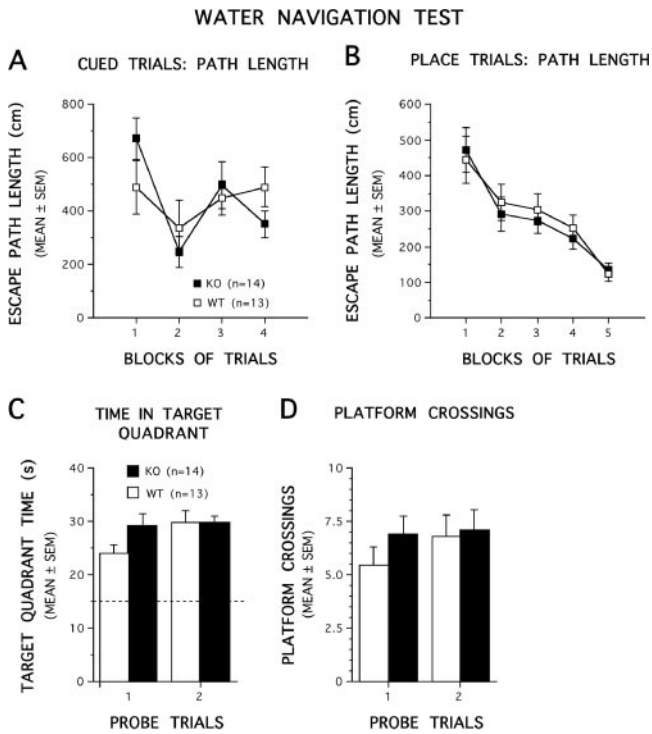


FIG. 2. CaMKK $\alpha$  KO mice performed similarly to WT littermates on several aspects of the Morris water navigation task. (A and B) Performance in terms of path length is depicted for the cued trials and for acquisition during the place condition as a function of blocks of trials. No differences were found between the groups at any point during either of the two tasks. (C and D) Retention performance on probe trials. No differences were found between KO and WT mice in terms of the amount of time the mice spent searching in the quadrant where the platform used to be located (target quadrant time [C]) or in the number of times the mice swam over the former platform location (platform crossings [D]). In panel C, the broken line represents the amount of time spent in the target quadrant that would be expected on the basis of chance alone.

type and effect of genotype by probe trial interaction,  $F_{1,25} < 1$ ). Significant effects of pool quadrant for the first and second probe trials ( $F_{3,75} = 41.11$  and  $P < 0.0005$  and  $F_{3,75} = 78.20$  and  $P < 0.0005$ , respectively) followed by significant comparisons between the target quadrant and each other quadrant (all  $P$  values  $< 0.003$ ) showed that each group had a “spatial bias” for the target quadrant during the first and second probe trials, in that each group spent significantly more time in the target quadrant compared to the other quadrants (not shown).

**Impaired long-term contextual fear memory in CaMKK $\alpha$ -deficient mice.** We have previously reported that CaMKIV/Gr KO mice showed a defect in fear memory (52). Since CaMKK $\alpha$  is postulated to act directly upstream of CaMKIV/Gr, we evaluated both contextual and cued fear memory in CaMKK $\alpha$  KO and WT mice during and after fear conditioning. During the conditioning session, the CaMKK $\alpha$  KO mice showed a significant deficit in context fear, as measured in the postshock freezing response ( $F_{1,19} = 4.93$  and  $P < 0.05$ ) (Fig. 3A). Both groups showed significant acquisition of fear across trials, as evidenced by increasing freezing during the postshock periods ( $F_{2,38} = 18.78$  and  $P < 0.0001$ ). The group effect and trial effect did not interact ( $F_{2,38} < 1$ ). In order to examine long-term fear

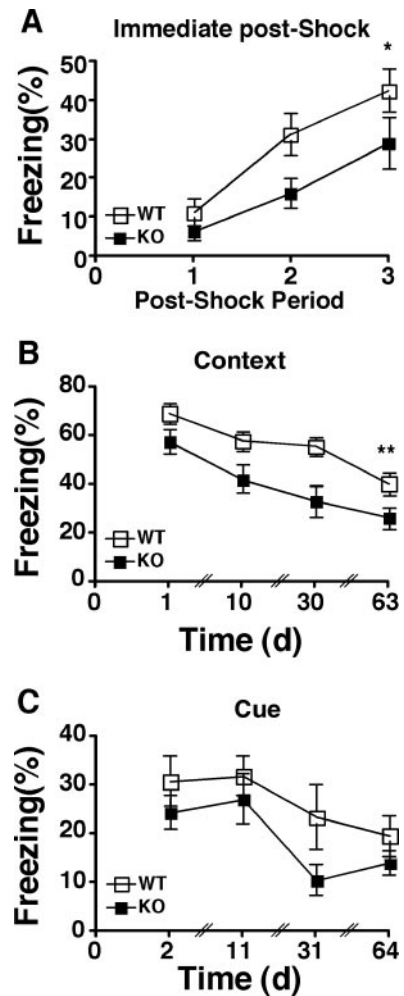


FIG. 3. Impaired contextual but not cued fear memory in CaMKK $\alpha$  KO mice. (A) Impaired contextual fear during training. Postshock freezing response was monitored for 30-s periods immediately following each of the three shocks. Values that were significantly different for WT and KO mice across periods are indicated (\*,  $P < 0.05$ ) (8 WT and 13 CaMKK $\alpha$  KO littermate mice). (B) Impaired contextual long-term fear memory. Following training, the mice in panel A were tested for contextual fear on days 1, 10, 30, and 63. Values that were significantly different for WT and KO mice across tests are indicated (\*\*,  $P < 0.01$ ). (C) Cued long-term fear memory. The same mice were tested for cued fear on days 2, 11, 31, and 64.  $P = 0.13$  across tests.

memory, context tests were conducted at 24 h, 10 days, 30 days, and 63 days after conditioning. CaMKK $\alpha$  KO mice exhibited significantly less freezing across tests than did the WT control mice ( $F_{1,19} = 7.72$  and  $P < 0.01$ ) (Fig. 3B). Both groups demonstrated extinction across test days ( $F_{3,57} = 20.41$  and  $P < 0.0001$ ), with no interaction between the genotype effect and the test day effect ( $F_{3,57} < 1$ ). Tone tests were conducted at 48 h, 11 days, 30 days, and 64 days after conditioning. CaMKK $\alpha$  KO and WT mice exhibited similar levels of freezing across tests ( $F_{1,19} = 2.48$  and  $P > 0.1$ ) (Fig. 3C). Both groups demonstrated extinction across test days ( $F_{3,57} = 8.52$  and  $P < 0.0001$ ), with no interaction between the genotype effect and the test day effect ( $F_{3,57} < 1$ ). Thus, genetic deletion of

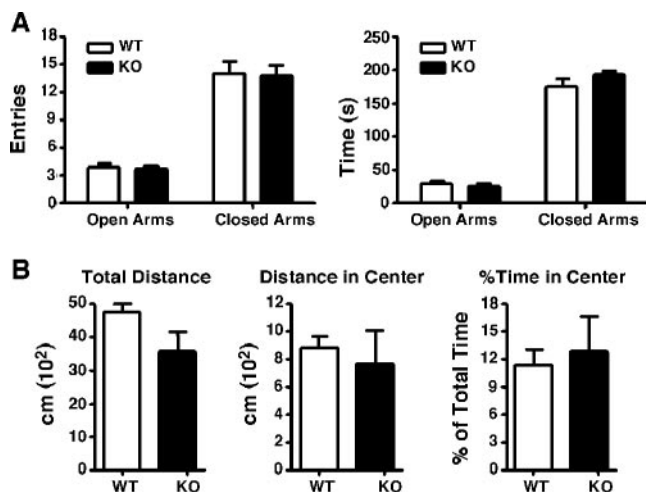


FIG. 4. CaMKK $\alpha$  KO mice exhibit normal anxiety-like behavior. (A) Elevated plus maze. The number of visits to the open and closed arms of the maze (left panel) and the time spent there (right panel) were similar between WT and CaMKK $\alpha$  KO mice. (B) Open field. There was no significant difference between WT and CaMKK $\alpha$  KO mice in the total distance traveled in the open field, in the distance traveled, or the time spent in the center (all measured over a 30-min period).

CaMKK $\alpha$  resulted in a significant but selective deficit in context fear.

**Normal locomotor behavior and anxiety in CaMKK $\alpha$ -deficient mice.** In addition to its impairment of fear memory, CaMKIV/Gr deficiency also resulted in decreased stress-induced anxiety-like behavior (46). To test the impact of CaMKK $\alpha$  deficiency on anxiety, we examined the performance of CaMKK $\alpha$  mice in the elevated plus maze. This is a well-validated test for anxiety-related behavior in mice in which an increase in anxiety correlates with a decrease in exploration of the open arms of the maze (32). Each animal was placed in the center portion of the elevated plus maze and allowed to explore freely for 5 min. The number of visits to the open and closed arms of the plus maze and the aggregate time spent there were recorded later from videotape. The number of entries into the open and closed arms of the plus maze were similar in WT and CaMKK $\alpha$  KO mice ( $t_{19} = 0.1526$  and  $P = 0.88$  and  $t_{19} = 0.1421$  and  $P = 0.88$ , respectively) (Fig. 4A). CaMKK $\alpha$  KO and WT mice also spent similar periods of time in both the open and close parts of the maze ( $t_{19} = 0.3764$  and  $P = 0.72$ ) and  $t_{19} = 1.176$  and  $P = 0.25$ , respectively) (Fig. 4A).

The behavior of mice in the open field test can also provide a measure of anxiety-like behavior. Decreased anxiety is associated with increased time spent and distance traveled in the center of the open field, an area that is normally aversive to rodents (40). There was no difference between CaMKK $\alpha$  mice and WT controls in the total distance traveled in the open field ( $t_{13} = 1.829$  and  $P = 0.09$ ), in the distance traveled in the center of the open field ( $t_{13} = 0.4486$  and  $P = 0.66$ ), or in the percentage of the total time on the open field platform spent in the center ( $t_{13} = 0.3198$  and  $P = 0.7542$ ) (Fig. 4B). Thus, the genetic deletion of CaMKK $\alpha$  had no effect on these standard measures of anxiety.

#### Impaired activation of downstream CaMKIV/Gr and CREB

**in CaMKK $\alpha$ -deficient mice subjected to fear conditioning.** Given the critical role of CaMKIV/Gr in fear memory formation, we next examined the status of CaMKIV/Gr activation in CaMKK $\alpha$  KO mice upon fear conditioning. Upstream CaMKK, including CaMKK $\alpha$  and CaMKK $\beta$ , activate CaMKIV/Gr by phosphorylating the regulatory threonine at position 196 (Thr196) in the activation loop of the kinase (7, 45). We employed an antibody against phospho-Thr196-CaMKIV/Gr (pCaMKIV/Gr) to examine the induction of CaMKIV/Gr Thr196 phosphorylation in brain sections of mice that have been subjected to the tone-shock conditioning regimen or those that were placed in the conditioning cage with no further manipulation as controls. Brain tissues examined were those previously implicated in context fear. Results revealed that fear conditioning was associated with enhanced pCaMKIV/Gr formation most prominently in the CA1 and CA3 areas of the hippocampus, the anterior cingulate cortex, and the somatosensory cortex, whereas weak staining was observed in the amygdala (Fig. 5 and data not shown). In comparison, pCaMKIV/Gr formation was significantly impaired in the CA1, CA3, and somatosensory cortex areas of similarly conditioned CaMKK $\alpha$  mutant mice ( $P = 0.014$ , 0.02, and 0.001, respectively). These results indicated that CaMKK $\alpha$  deficiency impaired the activation of CaMKIV/Gr in several neuronal areas involved in contextual fear memory formation.

We next evaluated the induction of CREB activation in CaMKK $\alpha$  KO mice in the context of fear conditioning by staining with phospho-serine 133 CREB antibody. Results revealed that pSer133-CREB staining was significantly increased in the dentate and CA3 regions of the hippocampus following fear conditioning. In contrast, pCREB staining was elevated at baseline in the dentate and CA3 regions of CaMKK $\alpha$  KO mice. Fear conditioning resulted in the loss of staining in those areas to levels below the baseline level of WT mice ( $P < 0.033$  and 0.01, respectively). pCREB staining was comparable at baseline in the lateral nucleus of the amygdala in WT and mutant mice. However, fear conditioning resulted in significantly increased pCREB formation in the lateral nucleus of the amygdala of WT but not mutant mice ( $P = 0.04$ ) (Fig. 6). These results indicated that activation of downstream components of the CaMK cascade previously implicated in fear memory formation, including CaMKIV/Gr and CREB, is compromised in CaMKK $\alpha$  KO mice undergoing fear conditioning.

**Normal basal synaptic transmission and LTP in CA1 neurons of CaMKK $\alpha$ -deficient mice.** To address the role of CaMKK $\alpha$  in synaptic plasticity, we examined LTP at the Schaffer collateral/CA1 synapse in the hippocampus. First, we examined the competency of basal synaptic transmission in hippocampal slices of WT and KO mice. Paired-pulse facilitation, a simple form of plasticity, in KO slices was similar to that of WT controls at different intervals measured (seven slices from five WT mice; seven slices from five KO mice) (Fig. 7A). No obvious difference in baseline excitatory postsynaptic currents (EPSPs) was observed in slices of WT and KO mice (data not shown). To test whether NMDA receptor-mediated responses may be affected in KO mice, we measured NMDA receptor-mediated EPSCs using whole-cell recording. Neurons were voltage clamped at  $-30$  mV, and NMDA receptor-mediated EPSCs were measured in the presence of CNQX (20  $\mu$ M), an

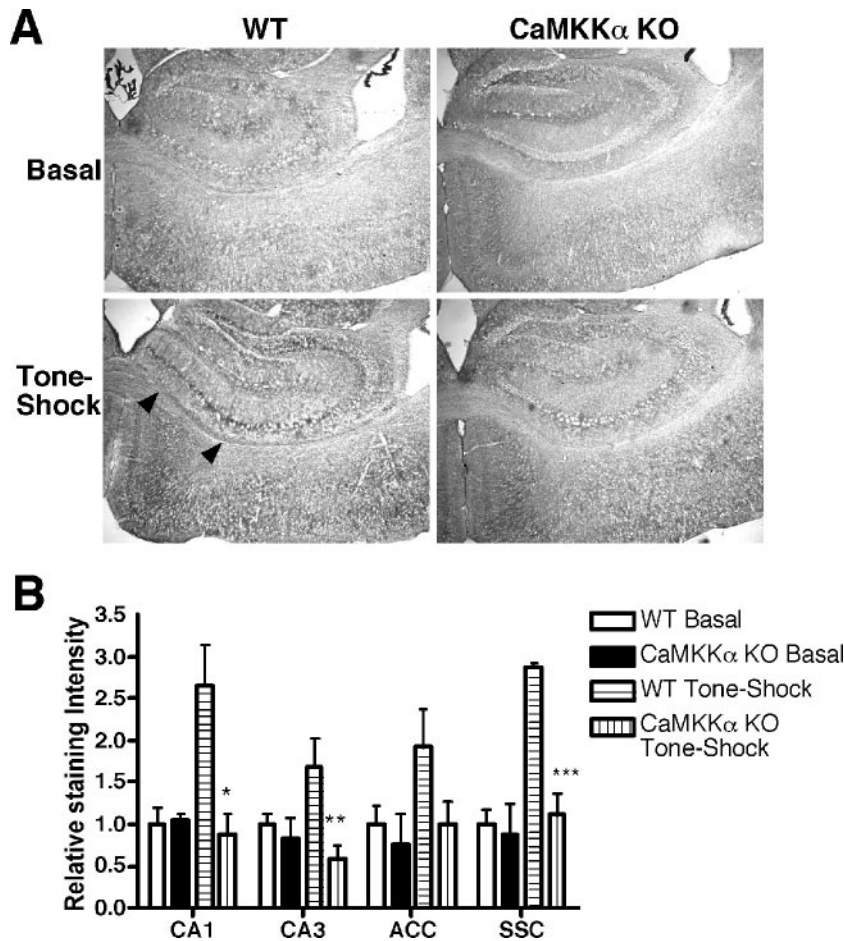


FIG. 5. Decreased pCaMKIV/Gr staining in brain subregions of fear-conditioned CaMKK $\alpha$  KO mice. (A) Representative sections ( $\times 4$  magnification) through the hippocampus of WT mice and CaMKK $\alpha$  KO mice placed in the training box with no further manipulation (Basal) or subjected to tone-shock paired training. Positive staining is associated with deposition of a dark precipitate after peroxidase staining (black arrowheads). (B) Quantification of pCaMKIV/Gr immunohistochemistry. Densitometric analysis of sections of WT and KO mice is shown (three or four mice for each group) (ACC, anterior cingulate cortex; SSC, somatosensory cortex [layer IV]). The average density of the WT basal group is normalized to 1 for each brain region. Values that are significantly different from the WT tone-shock group are indicated by asterisks (\*,  $P = 0.014$ ; \*\*,  $P = 0.02$ ; \*\*\*,  $P = 0.001$ ).

AMPA/kainate receptor antagonist and the input (stimulation intensity)-output (NMDA EPSC) function was recorded. We found that NMDA receptor-mediated responses in hippocampal slices of KO mice were not significantly different from those of WT mice (six slices from five WT mice; five slices from five KO mice) (Fig. 7B). Moreover, no significant difference was observed between the reversal potential of NMDA receptor-mediated responses in WT and KO slices (WT,  $16.5 \pm 2.3$  mV, five slices from five mice; KO,  $15.9 \pm 0.6$  mV, six slices from five mice).

Next we examined LTP induction in hippocampal slices of WT and KO mice. Tetanic stimulation (two trains, 100 Hz for 1 s/train, delivered at a 20-s interval) induced a similar amount of potentiation in slices of WT mice (eight slices from five WT mice,  $164.2\% \pm 26.0\%$  of control, comparing 40 to 45 min after tetanic stimulation to before the stimulation;  $P < 0.05$ ) and KO mice (three slices from three KO mice,  $181.5\% \pm 34.1\%$  of control;  $P < 0.05$ ) (Fig. 7C).

## DISCUSSION

The current scheme of a CaMK cascade composed of upstream activating kinases, including CaMKK $\alpha$  and CaMKK $\beta$ , and downstream effector kinases, including CaMKI and CaMKIV/Gr, raises questions concerning unique and redundant functions of the respective cascade component and the potential for specialized pairings of upstream and downstream kinases. In vitro studies using purified kinases revealed the two upstream kinases to be similar in their capacity to activate CaMKI and CaMKIV/Gr (2, 10, 49). Similarly, experiments on cell lines transfected with the respective upstream kinase revealed redundant capacity of CaMKK $\alpha$  and CaMKK $\beta$  to activate downstream CaMKIV/Gr- and CREB-dependent transcription (2, 49). In contrast, a more complex picture has emerged from studies on genetic mouse models deficient in individual components of the CaMK cascade, including CaMKIV/Gr, CaMKK $\beta$ , and now CaMKK $\alpha$ . CaMKIV/Gr deficiency was associated with a profound deficit in LTP and

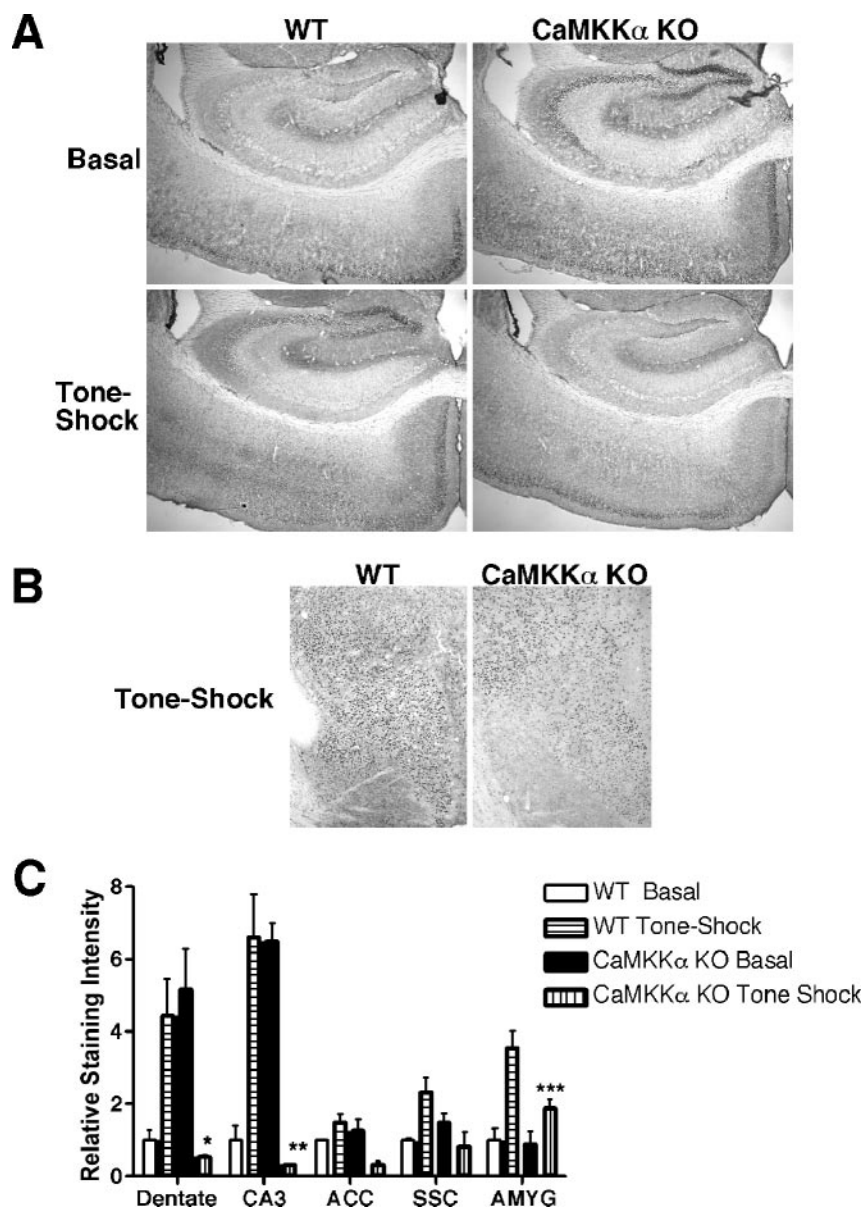


FIG. 6. Decreased pCREB staining in brain subregions of fear-conditioned CaMKK $\alpha$  KO mice. (A) Representative sections ( $\times 4$  magnification) through the hippocampus of WT mice and CaMKK $\alpha$  KO mice placed in the training box with no further manipulation (Basal) or subjected to tone-shock paired training. Positive cells are demonstrated by deposition of a dark nuclear precipitate after peroxidase staining. (B) Representative sections ( $\times 4$  magnification) through the amygdala of WT and CaMKK $\alpha$  KO mice following tone-shock paired training. (C) Quantification of pCREB immunohistochemistry. Densitometric analysis of sections of WT and KO mice is shown (three or four mice for each group). The average density of the WT Basal group is normalized to 1 for each brain region. Values that are significantly different from the respective tissue of the WT tone-shock group are indicated by asterisks (\*,  $P = 0.03$ ; \*\*,  $P = 0.01$ , \*\*\*,  $P = 0.04$ ). AMYG, amygdala.

CREB activation in several memory-related forebrain areas and impaired contextual and cued-fear LTM but normal spatial LTM. CaMKIV/Gr deficiency was also associated with defective stress-induced CREB activation and decreased stress-induced anxiety-like behavior (18). CaMKK $\beta$  deficiency impaired CREB activation upon spatial training and delayed the formation of spatial LTM but spared fear memory (38). In contrast, the present studies demonstrated that CaMKK $\alpha$  was dispensable for spatial memory but was revealed to promote contextual fear memory and CaMKIV/Gr and CREB activation upon fear conditioning. Unlike CaMKIV/Gr- and

CaMKK $\beta$ -deficient mice, CaMKK $\alpha$  KO mice exhibited normal hippocampal LTP. Collectively, these findings suggest divergent functions of the upstream components of the CaMK cascade in learning and memory.

Genetic deletion of CaMKK $\alpha$  resulted in relatively selective deficits in fear memory for context. The deletion did not disrupt normal levels of anxiety, as demonstrated in the elevated plus maze and open field preparations. Additionally, the deletion did not result in an overall disruption of fear learning per se. Tone testing indicated that the CaMKK $\alpha$  KO mice could acquire and express fear memory, even at remote testing points

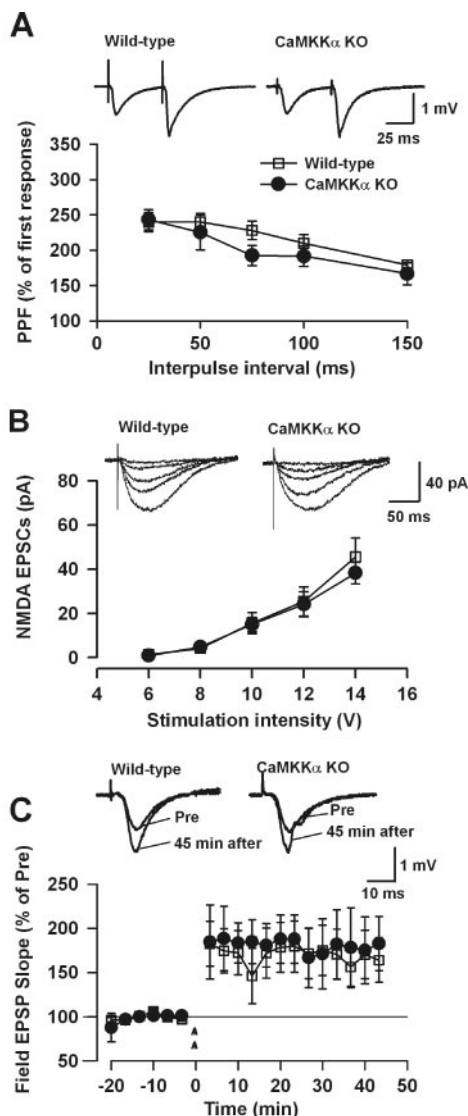


FIG. 7. CaMKK $\alpha$  KO mice show normal synaptic transmission and LTP. (A) WT and KO hippocampal slices show no significant difference in paired-pulse facilitation (PPF) of the EPSPs at various inter-pulse intervals (seven slices from five WT mice; seven slices from five KO mice). The insets show representative field EPSP traces with a paired-pulse interval of 50 ms. (B) WT and KO hippocampal slices show no significant difference in NMDA receptor-mediated EPSCs (six slices from five WT mice; five slices from five KO mice). The insets show example NMDA receptor-mediated EPSC traces at various stimulation intensities. (C) LTP is normal in CaMKK $\alpha$  KO mice. Two-train tetanic stimulation-induced LTP in the CA1 region of the hippocampus from WT mice (eight slices from five mice) and KO mice (three slices from three mice). The insets show representative field EPSP traces before and 45 min after tetanic stimulation.

following conditioning. In contrast, these same KO mice showed significant and persistent deficits in context fear. However, the possibility that CaMKK $\alpha$  deficiency imparts a subtler deficit in cued fear learning that would require testing of larger populations of mice to be uncovered cannot be ruled out. Intriguingly, the CaMKK $\alpha$  KO mice showed context fear deficits at every time point across repeated measures but showed no deficit at all in extinction of the freezing response across

tests. That is, the CaMKK $\alpha$  deletion may have weakened the formation or early consolidation of the context fear memory (as demonstrated by the immediate postshock freezing deficit and at the 24 h time point) but may also have left extinction learning mechanisms intact. Overall, the unique dissociations found with these animals include a deficit in fear learning but not in anxiety, a deficit in context fear but not in tone fear, and finally a deficit in acquisition/consolidation of context fear but not in extinction.

One caveat of the above behavioral studies is that they were carried out exclusively on male mice, leaving open the possibility of a sexual bias in the reported findings. There are well-characterized differences between male and female rodents in their acquisition of contextual fear learning. Females are slower to acquire contextual fear than males, although this difference disappears with repeated conditioning trials or longer context exposure prior to conditioning (34, 54). These differences, some of which may relate to estrous cycle-dependent changes in neurosteroid levels that impact the hippocampus, may reflect on the interaction between the sex of the animal and the genetic mutation(s) under study (55). Accordingly, the possibility that male CaMKK $\alpha$  KO mice more readily exhibit a deficit in contextual fear conditioning than their female counterparts cannot be ruled out, as this remains to be verified experimentally.

To date, much progress has been made in delineating the putative cellular substrates of learning and memory, specifically in the fear conditioning preparation. Critical roles have been revealed for CREB- and CaMKIV/Gr-related processes in fear acquisition and expression (6, 24, 26, 52). The findings here together with those of the aforementioned studies outline a linear relay within the CaMK cascade that is composed of CaMKK $\alpha$ , its downstream substrate CaMKIV/Gr, and the CaMKIV/Gr substrate CREB that is operative in fear memory. It should be noted that the deficit in phosphorylated CREB (pCREB) formation was selectively observed upon fear conditioning of CaMKK $\alpha$  KO mice but not at baseline, where the pCREB levels were either comparable to WT mice or even increased (such as in the hippocampus). This is in contrast to the more global deficit in pCREB formation observed in CaMKIV/Gr KO mice both at baseline and upon fear conditioning, reflective of the role of CaMKIV/Gr as a key CREB kinase (18, 52). These findings may be interpreted as suggesting that the role of the CaMKK $\alpha$  pathway in CREB activation is constrained to specific behavioral responses (e.g., fear memory).

The profound deficit in CREB activation in the hippocampus of CaMKK $\alpha$  KO mice upon fear conditioning is of particular significance given the critical role the hippocampus plays in processing the spatial context and relaying the information to the amygdala in the course of contextual fear conditioning (43). CREB-responsive element-dependent gene expression driven by CREB and related transcription factors is activated in the hippocampus upon contextual fear conditioning (23). Global CREB deficiency impairs contextual fear memory consolidation, as does antagonism of CREB-responsive element-dependent transcription in the hippocampus (3, 6, 13, 14, 39). Contextual fear conditioning up-regulates the expression of a number of genes in the hippocampus, several of which are targets of calcium/CREB signaling that have been implicated

in contextual fear memory consolidation (25, 30, 50). Of particular interest is brain-derived neurotrophic factor, which is induced in a calcium- and CREB-dependent manner and is up-regulated after contextual fear conditioning (15, 53). Brain-derived neurotrophic factor appears to selectively promote contextual fear memory consolidation; its deficiency or antagonism impairs contextual fear memory consolidation while sparing cued fear (29, 33). Other targets of calcium/CREB signaling include a number of immediate-early activation genes, such as *c-Fos*, which is induced by the CaMK cascade and whose deficiency impairs contextual fear conditioning (12, 18, 37). Further studies would be required to elucidate the contributions of these and other targets of the CaMK cascade to the observed deficit in contextual fear conditioning in CaMKK $\alpha$  KO mice.

Given that all the component kinases of the CaMK cascade share a strongly overlapping expression profile in forebrain tissues, these results can be interpreted to suggest that CaMKK $\alpha$  and CaMKK $\beta$  have both unique and redundant functions in activating downstream CaMK and/or other substrates, including CaMKIV/Gr. For example, the impairment of contextual fear memory in both CaMKIV/Gr and CaMKK $\alpha$  KO mice but not CaMKK $\beta$  KO mice argues for an upstream role of CaMKK $\alpha$  in regulating CaMKIV/Gr-dependent contextual fear learning. On the other hand, the absence in CaMKK $\alpha$  KO mice of LTP deficits common to CaMKK $\beta$  and CaMKIV/Gr KO mice suggests that CaMKK $\beta$  is the more relevant kinase in mediating LTP potentiation by CaMKIV/Gr.

In addition to activating downstream CaMKI and CaMKIV/Gr, both CaMKK $\alpha$  and CaMKK $\beta$  have been demonstrated to independently activate other signaling pathways. CaMKK $\alpha$  has been demonstrated to act as an Akt kinase that phosphorylates Akt on the regulatory threonine 308 residue, leading to its activation (57). Both CaMKK $\alpha$  and CaMKK $\beta$  have also been shown to phosphorylate and activate AMP kinase (4, 17, 19, 21, 56). The roles of these alternative pathways in promoting fear memory formation by CaMKK $\alpha$  are currently unclear and are the subject of ongoing investigation.

#### ACKNOWLEDGMENTS

Behavioral testing was carried out in the UCLA Behavioral Testing Core. We thank James Booth for animal care.

This work was supported by a pilot grant from the Alzheimer's Disease Research Center at Washington University in St. Louis (P50-AG05681) to T. A. Chatila and by an NIMH grant (RO1 MH62122) to M. S. Fanselow. M. Zhuo is supported by the EJLB-CIHR Michael Smith Chair in Neurosciences and Mental Health.

#### REFERENCES

- Anagnostaras, S. G., S. A. Josselyn, P. W. Frankland, and A. J. Silva. 2000. Computer-assisted behavioral assessment of Pavlovian fear conditioning in mice. *Learn. Mem.* 7:58–72.
- Anderson, K. A., R. L. Means, Q. H. Huang, B. E. Kemp, E. G. Goldstein, M. A. Selbert, A. M. Edelman, R. T. Freneau, and A. R. Means. 1998. Components of a calmodulin-dependent protein kinase cascade. Molecular cloning, functional characterization and cellular localization of Ca<sup>2+</sup>/calmodulin-dependent protein kinase beta. *J. Biol. Chem.* 273:31880–31889.
- Athos, J., S. Impey, V. V. Pineda, X. Chen, and D. R. Storm. 2002. Hippocampal CRE-mediated gene expression is required for contextual memory formation. *Nat. Neurosci.* 5:1119–1120.
- Birnbaum, M. J. 2005. Activating AMP-activated protein kinase without AMP. *Mol. Cell* 19:289–290.
- Blaeser, F., N. Ho, R. Prywes, and T. A. Chatila. 2000. Ca<sup>2+</sup>-dependent gene expression mediated by MEF2 transcription factors. *J. Biol. Chem.* 275:197–209.
- Bourtchuladze, R., B. Frenguelli, J. Blendy, D. Cioffi, G. Schutz, and A. J. Silva. 1994. Deficient long-term memory in mice with a targeted mutation of the cAMP-responsive element-binding protein. *Cell* 79:59–68.
- Chatila, T., K. A. Anderson, N. Ho, and A. R. Means. 1996. A unique phosphorylation-dependent mechanism for the activation of Ca<sup>2+</sup>/calmodulin-dependent protein kinase type IV/Gr. *J. Biol. Chem.* 271:21542–21548.
- Chawla, S., G. E. Hardingham, D. R. Quinn, and H. Bading. 1998. CBP: a signal-regulated transcriptional coactivator controlled by nuclear calcium and CaM kinase IV. *Science* 281:1505–1509.
- Corcoran, E. E., and A. R. Means. 2001. Defining Ca<sup>2+</sup>/calmodulin-dependent protein kinase cascades in transcriptional regulation. *J. Biol. Chem.* 276:2975–2978.
- Edelman, A. M., K. I. Mitchelhill, M. A. Selbert, K. A. Anderson, S. S. Hook, D. Stapleton, E. G. Goldstein, A. R. Means, and B. E. Kemp. 1996. Multiple Ca<sup>2+</sup>-calmodulin-dependent protein kinase kinases from rat brain. Purification, regulation by Ca<sup>2+</sup>-calmodulin, and partial amino acid sequence. *J. Biol. Chem.* 271:10806–10810.
- Fanselow, M. S. 1980. Conditioned and unconditional components of post-shock freezing. *Pavlov. J. Biol. Sci.* 15:177–182.
- Fleischmann, A., O. Hvalby, V. Jensen, T. Strekalova, C. Zacher, L. E. Layer, A. Kvello, M. Reschke, R. Spanagel, R. Sprengel, E. F. Wagner, and P. Gass. 2003. Impaired long-term memory and NR2A-type NMDA receptor-dependent synaptic plasticity in mice lacking *c-Fos* in the CNS. *J. Neurosci.* 23:9116–9122.
- Frankland, P. W., S. A. Josselyn, S. G. Anagnostaras, J. H. Kogan, E. Takahashi, and A. J. Silva. 2004. Consolidation of CS and US representations in associative fear conditioning. *Hippocampus* 14:557–569.
- Graves, L., A. Dalvi, I. Lucki, J. A. Blendy, and T. Abel. 2002. Behavioral analysis of CREB alphas mutation on a B6/129 F1 hybrid background. *Hippocampus* 12:18–26.
- Hall, J., K. L. Thomas, and B. J. Everitt. 2000. Rapid and selective induction of BDNF expression in the hippocampus during contextual learning. *Nat. Neurosci.* 3:533–535.
- Hanks, S. K., A. M. Quinn, and T. Hunter. 1988. The protein kinase family: conserved features and deduced phylogeny of the catalytic domains. *Science* 241:42–52.
- Hawley, S. A., D. A. Pan, K. J. Mustard, L. Ross, J. Bain, A. M. Edelman, B. G. Frenguelli, and D. G. Hardie. 2005. Calmodulin-dependent protein kinase beta is an alternative upstream kinase for AMP-activated protein kinase. *Cell Metab.* 2:9–19.
- Ho, N., J. A. Liauw, F. Blaeser, F. Wei, S. Hanissian, L. M. Muglia, D. F. Wozniak, A. Nardi, K. L. Arvin, D. M. Holtzman, D. J. Linden, M. Zhuo, L. J. Muglia, and T. A. Chatila. 2000. Impaired synaptic plasticity and cAMP response element-binding protein activation in Ca<sup>2+</sup>/calmodulin-dependent protein kinase type IV/Gr-deficient mice. *J. Neurosci.* 20:6459–6472.
- Hong, S. P., M. Momcilovic, and M. Carlson. 2005. Function of mammalian LKB1 and Ca<sup>2+</sup>/calmodulin-dependent protein kinase alpha as Snf1-activating kinases in yeast. *J. Biol. Chem.* 280:21804–21809.
- Hu, S. C., J. Chrivia, and A. Ghosh. 1999. Regulation of CBP-mediated transcription by neuronal calcium signaling. *Neuron* 22:799–808.
- Hurley, R. L., K. A. Anderson, J. M. Franzone, B. E. Kemp, A. R. Means, and L. A. Witters. 2005. The Ca<sup>2+</sup>/calmodulin-dependent protein kinase kinases are AMP-activated protein kinase kinases. *J. Biol. Chem.* 280:29060–29066.
- Impey, S., A. L. Fong, Y. Wang, J. R. Cardinaux, D. M. Fass, K. Obrietan, G. A. Wayman, D. R. Storm, T. R. Soderling, and R. H. Goodman. 2002. Phosphorylation of CBP mediates transcriptional activation by neural activity and CaM kinase IV. *Neuron* 34:235–244.
- Impey, S., D. M. Smith, K. Obrietan, R. Donahue, C. Wade, and D. R. Storm. 1998. Stimulation of cAMP response element (CRE)-mediated transcription during contextual learning. *Nat. Neurosci.* 1:595–601.
- Josselyn, S. A., C. Shi, W. A. Carlezon, Jr., R. L. Neve, E. J. Nestler, and M. Davis. 2001. Long-term memory is facilitated by cAMP response element-binding protein overexpression in the amygdala. *J. Neurosci.* 21:2404–2412.
- Keeley, M. B., M. A. Wood, C. Isiegas, J. Stein, K. Hellman, S. Hannenhalli, and T. Abel. 2006. Differential transcriptional response to nonassociative and associative components of classical fear conditioning in the amygdala and hippocampus. *Learn. Mem.* 13:135–142.
- Kida, S., S. A. Josselyn, S. P. de Ortiz, J. H. Kogan, I. Chevere, S. Masushige, and A. J. Silva. 2002. CREB required for the stability of new and reactivated fear memories. *Nat. Neurosci.* 5:348–355.
- Kimura, Y., E. E. Corcoran, K. Eto, K. Gengyo-Ando, M. A. Muramatsu, R. Kobayashi, J. H. Freedman, S. Mitani, M. Hagiwara, A. R. Means, and H. Tokumitsu. 2002. A CaMK cascade activates CRE-mediated transcription in neurons of *Caenorhabditis elegans*. *EMBO Rep.* 3:962–966.
- Ko, S. W., H. S. Ao, A. G. Mendel, C. S. Qiu, F. Wei, J. Milbrandt, and M. Zhuo. 2005. Transcription factor Egr-1 is required for long-term fear memory and anxiety. *Sheng Li Xue Bao* 57:421–432.
- Lee, J. L., B. J. Everitt, and K. L. Thomas. 2004. Independent cellular processes for hippocampal memory consolidation and reconsolidation. *Science* 304:839–843.
- Levenson, J. M., S. Choi, S. Y. Lee, Y. A. Cao, H. J. Ahn, K. C. Worley, M. Pizzi, H. C. Liou, and J. D. Sweatt. 2004. A bioinformatics analysis of

- memory consolidation reveals involvement of the transcription factor c-rel. *J. Neurosci.* **24**:3933–3943.
31. **Liau, J., L. J. Wu, and M. Zhuo.** 2005. Calcium-stimulated adenylyl cyclases required for long-term potentiation in the anterior cingulate cortex. *J. Neurophysiol.* **94**:878–882.
  32. **Lister, R. G.** 1987. The use of a plus-maze to measure anxiety in the mouse. *Psychopharmacology (Berlin)* **92**:180–185.
  33. **Liu, I. Y., W. E. Lyons, L. A. Mamounas, and R. F. Thompson.** 2004. Brain-derived neurotrophic factor plays a critical role in contextual fear conditioning. *J. Neurosci.* **24**:7958–7963.
  34. **Maren, S., B. De Oca, and M. S. Fanselow.** 1994. Sex differences in hippocampal long-term potentiation (LTP) and Pavlovian fear conditioning in rats: positive correlation between LTP and contextual learning. *Brain Res.* **661**:25–34.
  35. **Matthews, R. P., C. R. Guthrie, L. M. Wailes, X. Zhao, A. R. Means, and G. S. McKnight.** 1994. Calcium/calmodulin-dependent protein kinase types II and IV differentially regulate CREB-dependent gene expression. *Mol. Cell. Biol.* **14**:6107–6116.
  36. **McKinsey, T. A., C. L. Zhang, J. Lu, and E. N. Olson.** 2000. Signal-dependent nuclear export of a histone deacetylase regulates muscle differentiation. *Nature* **408**:106–111.
  37. **Miranti, C. K., D. D. Ginty, G. Huang, T. Chatila, and M. E. Greenberg.** 1995. Calcium activates serum response factor-dependent transcription by a Ras- and Elk-1-independent mechanism that involves a Ca<sup>2+</sup>/calmodulin-dependent kinase. *Mol. Cell. Biol.* **15**:3672–3684.
  38. **Peters, M., K. Mizuno, L. Ris, M. Angelo, E. Godaux, and K. P. Giese.** 2003. Loss of Ca<sup>2+</sup>/calmodulin kinase kinase beta affects the formation of some, but not all, types of hippocampus-dependent long-term memory. *J. Neurosci.* **23**:9752–9760.
  39. **Pittenger, C., Y. Y. Huang, R. F. Paletzki, R. Bourchouladze, H. Scanlin, S. Vronskaya, and E. R. Kandel.** 2002. Reversible inhibition of CREB/ATF transcription factors in region CA1 of the dorsal hippocampus disrupts hippocampus-dependent spatial memory. *Neuron* **34**:447–462.
  40. **Ramos, A., O. Berton, P. Mormede, and F. Chaouloff.** 1997. A multiple-test study of anxiety-related behaviours in six inbred rat strains. *Behav. Brain Res.* **85**:57–69.
  41. **Ribar, T. J., R. M. Rodriguiz, L. Khiroug, W. C. Wetsel, G. J. Augustine, and A. R. Means.** 2000. Cerebellar defects in Ca<sup>2+</sup>/calmodulin kinase IV-deficient mice. *J. Neurosci.* **20**:RC107.
  42. **Sakagami, H., M. Umemiya, S. Saito, and H. Kondo.** 2000. Distinct immunohistochemical localization of two isoforms of Ca<sup>2+</sup>/calmodulin-dependent protein kinase kinases in the adult rat brain. *Eur. J. Neurosci.* **12**:89–99.
  43. **Sanders, M. J., B. J. Wiltgen, and M. S. Fanselow.** 2003. The place of the hippocampus in fear conditioning. *Eur. J. Pharmacol.* **463**:217–223.
  44. **Schmitt, J. M., E. S. Guire, T. Saneyoshi, and T. R. Soderling.** 2005. Calmodulin-dependent kinase kinase/calmodulin kinase I activity gates extra-cellular-regulated kinase-dependent long-term potentiation. *J. Neurosci.* **25**:1281–1290.
  45. **Selbert, M. A., K. A. Anderson, Q. H. Huang, E. G. Goldstein, A. R. Means, and A. M. Edelman.** 1995. Phosphorylation and activation of Ca<sup>2+</sup>-calmodulin-dependent protein kinase IV by Ca<sup>2+</sup>-calmodulin-dependent protein kinase Ia kinase. Phosphorylation of threonine 196 is essential for activation. *J. Biol. Chem.* **270**:17616–17621.
  46. **Shum, F. W., S. W. Ko, Y. S. Lee, B. K. Kaang, and M. Zhuo.** 2005. Genetic alteration of anxiety and stress-like behavior in mice lacking CaMKIV. *Mol. Pain* **1**:22.
  47. **Soderling, T. R.** 1999. The Ca-calmodulin-dependent protein kinase cascade. *Trends Biochem. Sci.* **24**:232–236.
  48. **Sun, P., H. Enslin, P. S. Myung, and R. A. Maurer.** 1994. Differential activation of CREB by Ca<sup>2+</sup>/calmodulin-dependent protein kinases type II and type IV involves phosphorylation of a site that negatively regulates activity. *Genes Dev.* **8**:2527–2539.
  49. **Tokumitsu, H., H. Enslin, and T. R. Soderling.** 1995. Characterization of a Ca<sup>2+</sup>/calmodulin-dependent protein kinase cascade. Molecular cloning and expression of calcium/calmodulin-dependent protein kinase kinase. *J. Biol. Chem.* **270**:19320–19324.
  50. **von Herten, L. S., and K. P. Giese.** 2005. Memory reconsolidation engages only a subset of immediate-early genes induced during consolidation. *J. Neurosci.* **25**:1935–1942.
  51. **Wayman, G. A., S. Kaeck, W. F. Grant, M. Davare, S. Impey, H. Tokumitsu, N. Nozaki, G. Banker, and T. R. Soderling.** 2004. Regulation of axonal extension and growth cone motility by calmodulin-dependent protein kinase I. *J. Neurosci.* **24**:3786–3794.
  52. **Wei, F., C. S. Qiu, J. Liauw, D. A. Robinson, N. Ho, T. Chatila, and M. Zhuo.** 2002. Calcium calmodulin-dependent protein kinase IV is required for fear memory. *Nat. Neurosci.* **5**:573–579.
  53. **West, A. E., W. G. Chen, M. B. Dalva, R. E. Dolmetsch, J. M. Kornhauser, A. J. Shaywitz, M. A. Takasu, X. Tao, and M. E. Greenberg.** 2001. Calcium regulation of neuronal gene expression. *Proc. Natl. Acad. Sci. USA* **98**:11024–11031.
  54. **Wiltgen, B. J., M. J. Sanders, N. S. Behne, and M. S. Fanselow.** 2001. Sex differences, context preexposure, and the immediate shock deficit in Pavlovian context conditioning with mice. *Behav. Neurosci.* **115**:26–32.
  55. **Wiltgen, B. J., M. J. Sanders, C. Ferguson, G. E. Homanics, and M. S. Fanselow.** 2005. Trace fear conditioning is enhanced in mice lacking the delta subunit of the GABAA receptor. *Learn. Mem.* **12**:327–333.
  56. **Woods, A., K. Dickerson, R. Heath, S. P. Hong, M. Momcilovic, S. R. Johnstone, M. Carlson, and D. Carling.** 2005. Ca<sup>2+</sup>/calmodulin-dependent protein kinase kinase-beta acts upstream of AMP-activated protein kinase in mammalian cells. *Cell Metab.* **2**:21–33.
  57. **Yano, S., H. Tokumitsu, and T. R. Soderling.** 1998. Calcium promotes cell survival through CaM-K kinase activation of the protein-kinase-B pathway. *Nature* **396**:584–587.